Supplementary Information (SI) for Catalysis Science & Technology.

Selective CO Production from CO_2 over Metal Catalyst Supported on Perovskite Oxide under the Presence of Excess Hydrogen

Keigo Tashiro, [a,b,c] Shinnosuke Sekizawa,[a] Wataru Doi,[b] Hikaru Konno,[a] Kensuke Izutani,[a] Takayuki Furukawa,[a] Akihide Yanagita,[a] and Shigeo Satokawa*[a,b]

a Graduate School of Science and Technology, Seikei University, 3-3-1 Kichijoji-Kitamachi, Musashino, Tokyo 180-8633, Japan.

b Faculty of Science and Technology, Seikei University, 3-3-1 Kichijoji-Kitamachi, Musashino, Tokyo 180-8633, Japan.

c College of Engineering, Academic Institute, Shizuoka University, 3-5-1 Johoku, Chuo-ku, Hamamatsu-shi, Shizuoka 432-8561, Japan.

Corresponding author
Prof. Shigeo Satokawa
E-mail: satokawa@st.seikei.ac.jp

Abstract:

Hydrogenation of carbon dioxide (CO_2) to liquid fuels via industrial catalytic reaction is a most effective strategy for the realization of carbon neutrality. The subsequential reaction system of reverse water gas shift (RWGS) reaction followed by Fischer–Tropsch synthesis is promising way to achieve this, hence the development of catalysts with high conversion and selectivity for the former RWGS is required. We succeeded in the conversion of CO_2 to carbon monoxide (CO) with 100% of selectivity in gas phase by using platinum-loaded perovskite oxide support composed of barium and zirconium in which 10% of zirconium was substituted with yttrium ($Pt/BaZr_{0.9}Y_{0.1}O_{3-\delta}$, Pt/BZY10) at 500 °C in the gas stream with H_2/CO_2 = 3. On the other hand, ruthenium-loaded catalyst (Ru/BZY10) afforded not only CO but also methane (CH_4) as gaseous product. Kinetic analysis demonstrated that the activation energy was identical for both catalysts, while Fourier transform infrared spectroscopy clarified that the surface-adsorbed methoxy group as reaction intermediate was generated only in case of Ru/BZY10, which indicated the ability of the loaded-metal for the dissociative adsorption of hydrogen. The present research is expected to contribute a new methodology for the preparation of catalysts toward RWGS reaction and a quite important insight for the realization of the carbon neutrality.

Supporting methods

Materials

Ammonium oxalate monohydrate ($(NH_4)_2(COO)_2 \cdot H_2O$), barium nitrate ($Ba(NO_3)_2$), zirconyl nitrate dihydrate ($ZrO(NO_3)_2 \cdot 2H_2O$), copper(II) nitrate trihydrate ($Cu(NO_3)_2 \cdot 3H_2O$), iron(III) nitrate nonahydrate ($Fe(NO_3)_3 \cdot 9H_2O$), manganese(II) nitrate hexahydrate ($Mn(NO_3)_2 \cdot 6H_2O$), and potassium bromide (KBr) were acquired from FUJIFILM Wako Pure Chemical Corp. Yttrium(III) nitrate hexahydrate ($Y(NO_3)_3 \cdot 6H_2O$), nickel(II) nitrate hexahydrate ($Ni(NO_3)_2 \cdot 6H_2O$), and silver Nitrate ($AgNO_3$) were purchased from KANTO CHEMICAL Co. Inc. Cobalt(II) nitrate hexahydrate ($Co(NO_3)_2 \cdot 6H_2O$) was obtained from Sigma-Aldrich Japan. Diamminedinitritoplatinum(II) ($[Pt(NH_3)_2(NO_2)_2]$) in nitric acid (HNO_3), ruthenium(III) nitrate ($Ru(NO_3)_3$)aqueous solution and palladium(II) nitrate ($Pd(NO_3)_2$) aqueous solution were afforded by TANAKA Kikinzoku Kogyo K. K. Iridium(IV) nitrate ($Ir(NO_3)_4$) aqueous solution and rhodium(III) nitrate ($Rh(NO_3)_3$) aqueous solution were purchased from Furuya Metal Co., Ltd.

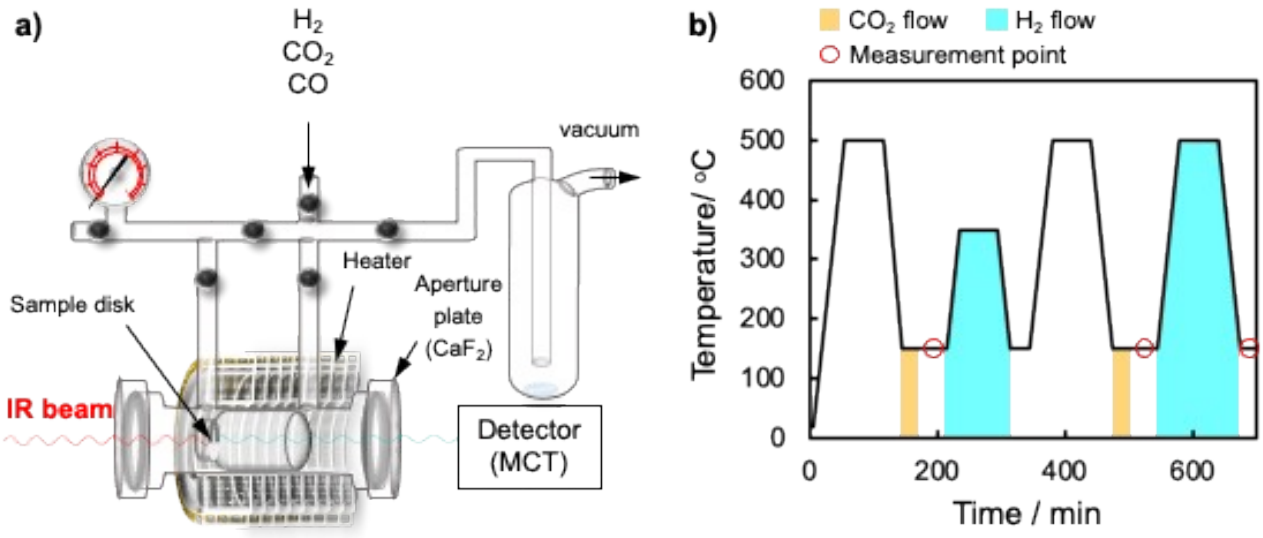

Figure S1. (**a**) Schematic representation of analytical system of in-situ FT-IR. (**b**) Time profile of temperature and gas flow on the in-situ FT-IR analysis.

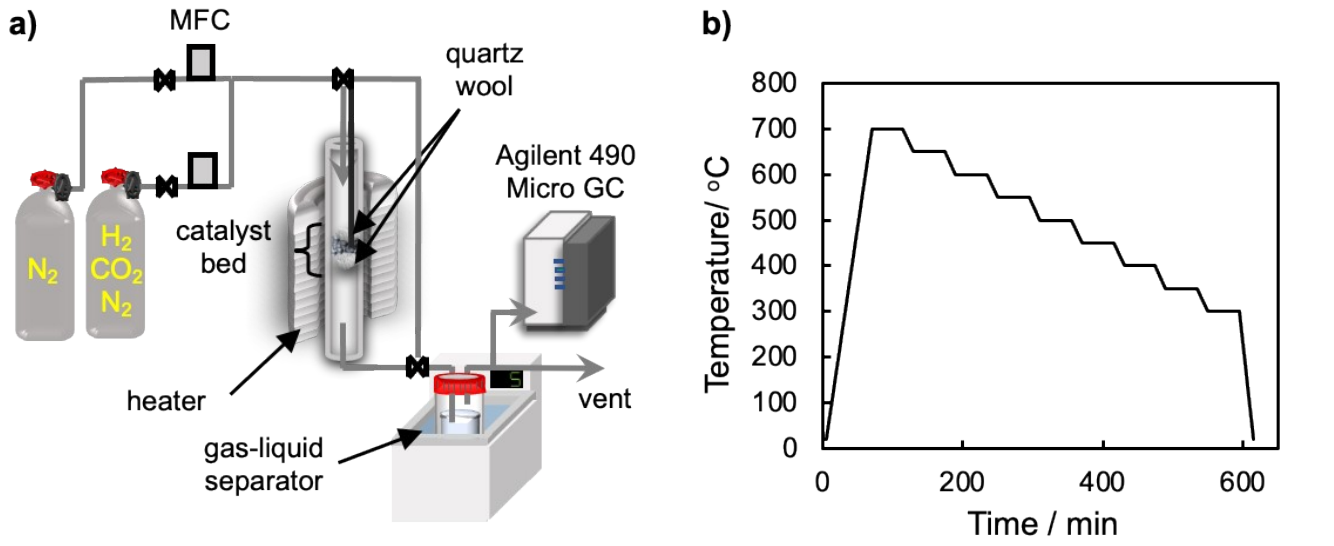

Figure S2. (**a**) Schematic representation of catalytic performance evaluation system. (**b**) Time course of temperature during catalytic evaluation upon CO_2 hydrogenation.

Supporting Results

Table S1. Element compositions and Brunauer–Emmett–Teller surface areas of 0.1 wt%-M/BZY10 (M= Mn, Fe, Co, Ni, Cu, Ru, Rh, Pd, Ag, Ir, and Pt).

Sample	Element composition / wt% *a				S^{BET} / $m^2\ g^{-1}$
	Ba	Zr	Y	Loaded metal	
BZY10	55.24	40.24	4.19	–	15.2
Mn/BZY10	55.51	40.10	4.17	0.21	16.9
Fe/BZY10	55.38	40.22	4.18	0.09	16.9
Co/BZY10	55.50	42.57	4.44	0.19	14.7
Ni/BZY10	52.80	43.41	4.51	0.13	14.4
Cu/BZY10	51.94	41.42	4.30	0.21	15.9
Ru/BZY10	53.06	41.95	4.36	0.08	113.9
Rh/BZY10	54.30	41.32	4.29	0.07	14.5
Pd/BZY10	55.22	40.48	4.20	0.09	14.8
Ag/BZY10	54.23	41.45	4.32	0.00 *b	16.2
Ir/BZY10	55.65	41.77	4.34	0.23	14.2
Pt/BZY10	57.05	38.75	4.03	0.16	17.0

*a Element composition was identified by X-ray fluorescence (XRF) measurements with fundamental parameter method. On the preparation, all metal precursors were added to the reaction solution with 0.1 wt% of metal amount to BZY10.

*b Not detectable due to the usage of silver tube in the apparatus.

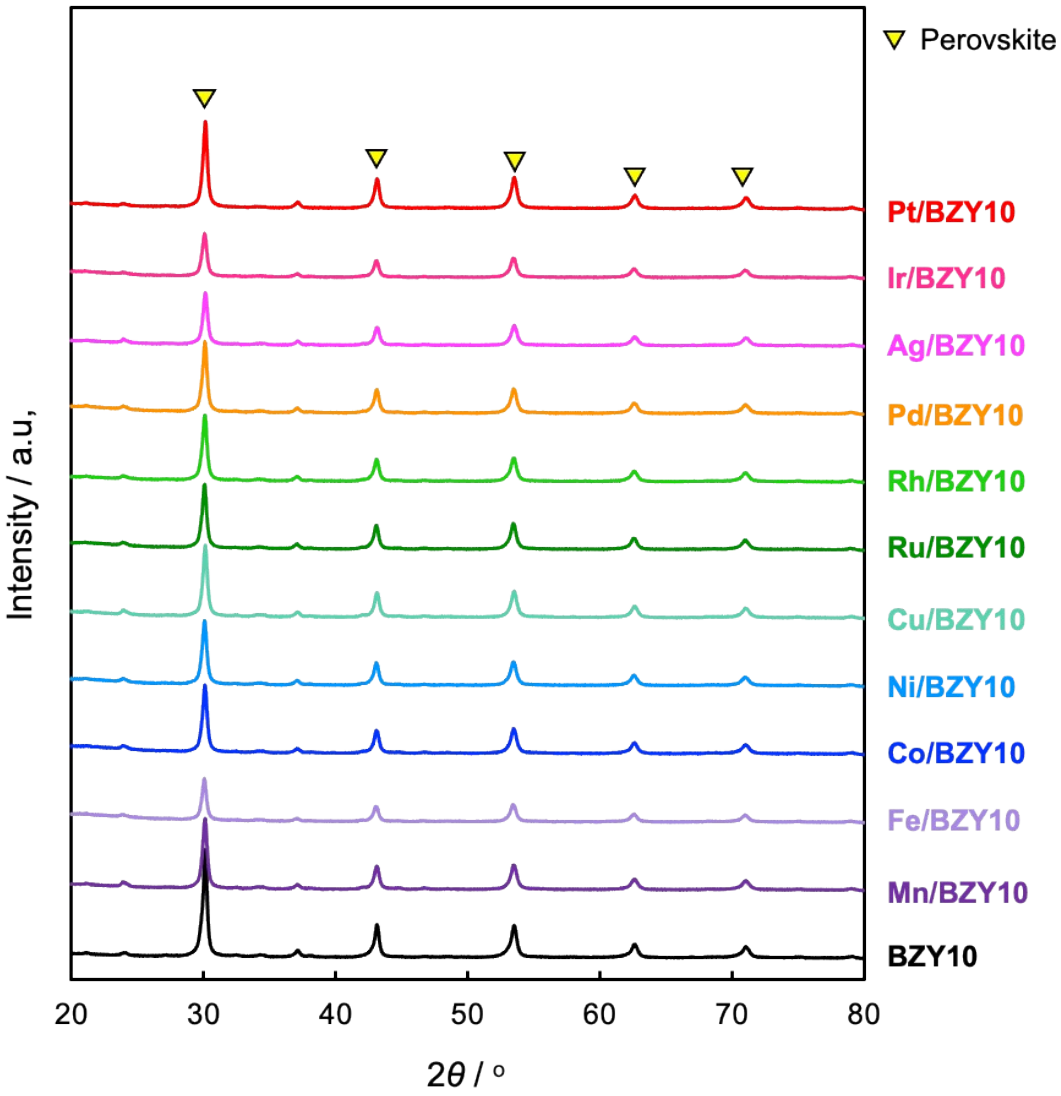

Figure S3. XRD patterns of 0.1 wt%-M/BZY10 (M = Mn, Fe, Co, Ni, Cu, Ru, Rh, Pd, Ag, Ir, and Pt).

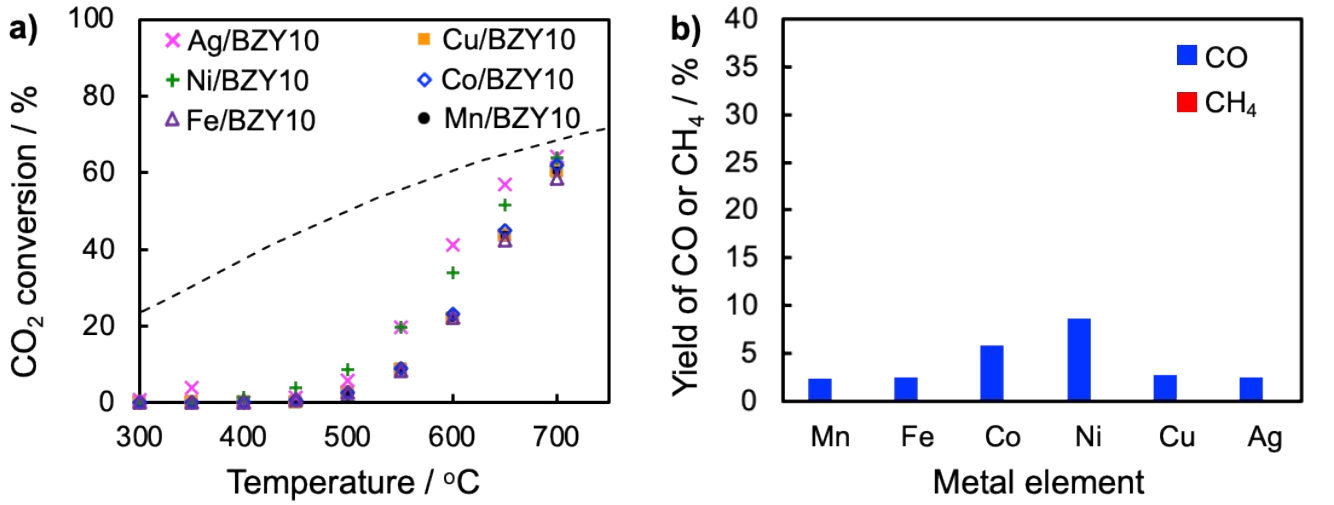

Figure S4. (**a**) CO_2 conversion as a function of reaction temperature on the RWGS reaction under the gas stream of H_2/CO_2 = 3 over 0.1 wt%-M/BZY10 (M = Mn, Fe, Co, Ni, Cu, and Ag). The black dashed line indicates theoretical equilibrium conversion of CO_2 upon RWGS reaction under gas composition of H_2/CO_2 =3. (**b**) Yields of CO and CH_4 resulting from the RWGS reaction performed at 500 °C under the gas stream of H_2/CO_2 = 3 over 0.1 wt%-M/BZY10 (M = Mn, Fe, Co, Ni, Cu, and Ag). No CH_4 was generated for all samples.

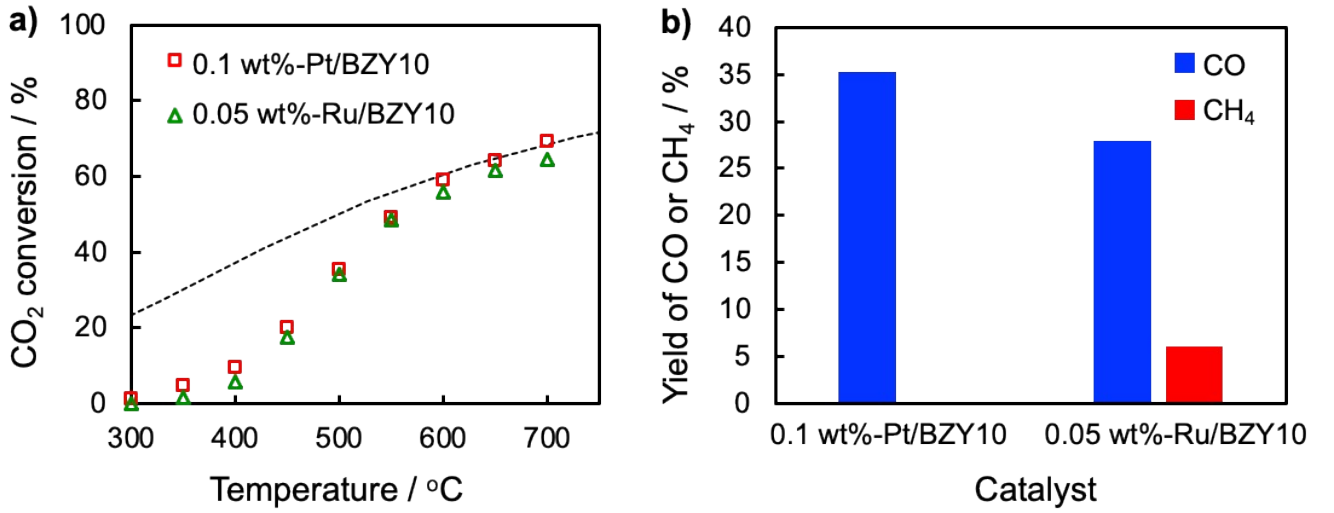

Figure S5. (**a**) CO_2 conversion as a function of reaction temperature on the RWGS reaction under the gas stream of H_2/CO_2 = 3 over 0.1 wt%-Pt/BZY10 and 0.05 wt%-Ru/BZY10. The black dashed line indicates theoretical equilibrium conversion of CO_2 upon RWGS reaction under gas composition of H_2/CO_2 =3. (**b**) Yields of CO and CH_4 resulting from the RWGS reaction performed at 500 °C under the gas stream of H_2/CO_2 = 3 over 0.1 wt%-Pt/BZY10 and 0.05 wt%-Ru/BZY10. Here, 0.1 wt% of Pt and 0.05 wt% of Ru correspond to 5.0×10^{-6} mol.

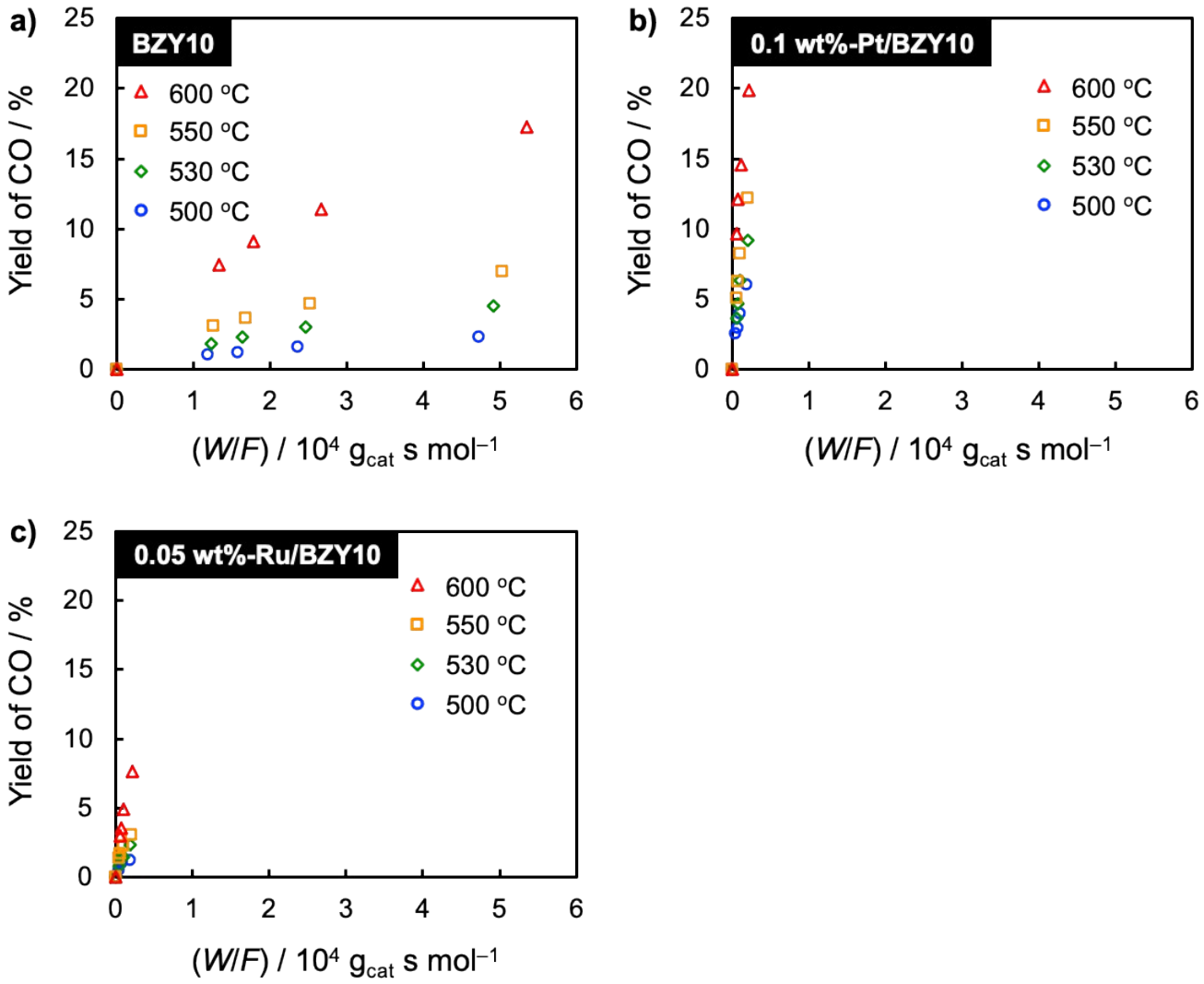

Figure S6. (**a**–**c**) Identically-scaled plots for the yield of CO against *W*/*F* resulting from RWGS reaction under the stream of the reactant gas with H_2/CO_2 = 3 at 500, 530, 550 and 600 °C over (**a**) BZY10, (**b**) 0.1 wt%-Pt/BZY10, and (**c**) 0.05 wt%-Ru/BZY10; the amount of metal was adjusted to 5.0×10^{-6} mol.

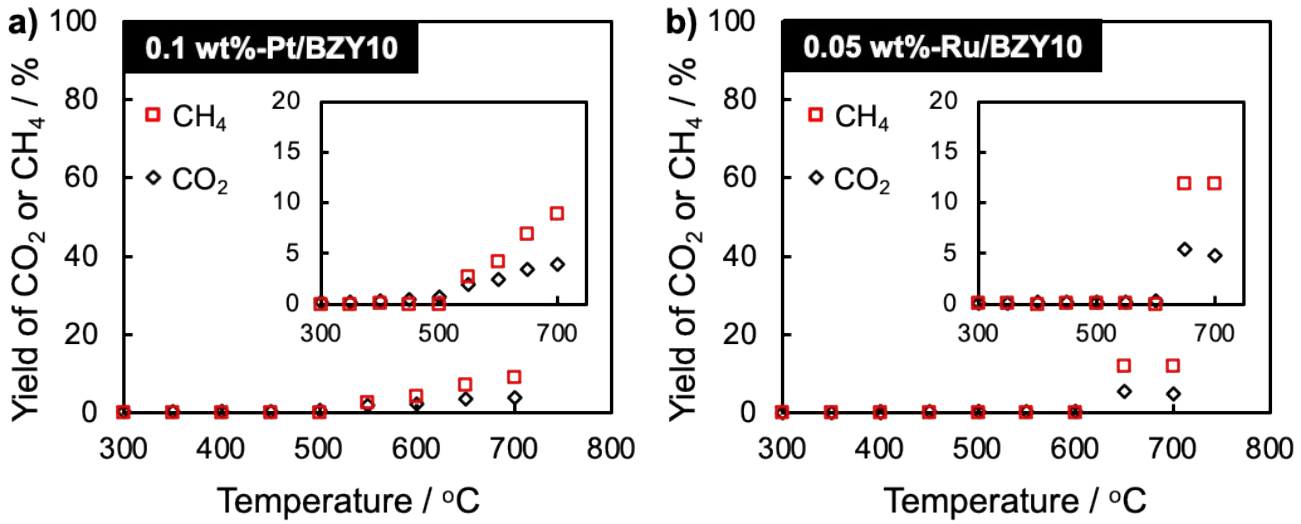

Figure S7. (**a**,**b**) The yields of CO_2 and CH_4 against temperature on the catalytic reaction under gas stream of H_2/CO = 3 over (**a**) 0.1 wt%-Pt/BZY10 and (**b**) 0.05 wt%-Ru/BZY10.

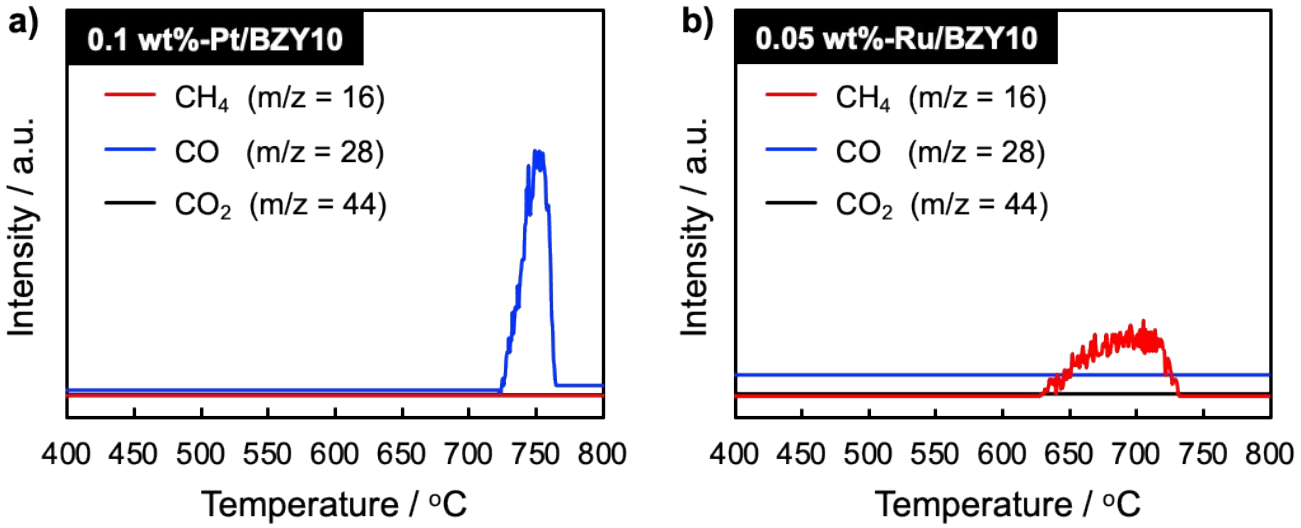

Figure S8. (**a**,**b**) Chromatograms of outlet gases after H_2-TPR of CO_2-adsorbed-catalyst; (**a**) 0.1 wt%-Pt/BZY10 and (**b**) 0.05 wt%-Ru/BZY10.

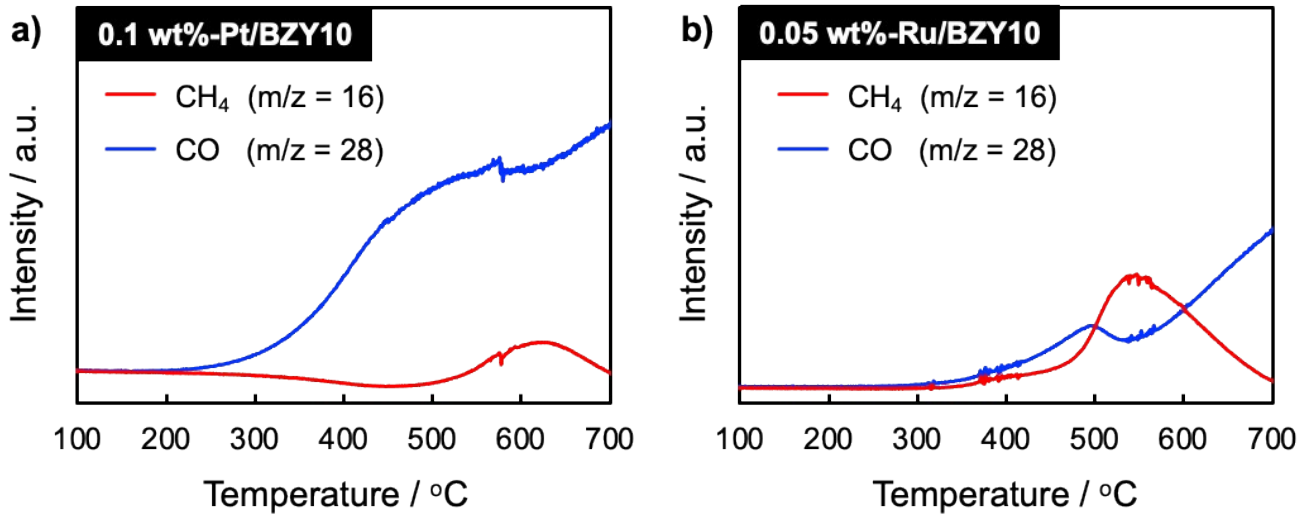

Figure S9. (**a**,**b**) Chromatograms of outlet gases during temperature elevation under gas flow (H_2/CO_2 = 3) and same condition to H_2-TPR except for gas composition over (**a**) 0.1 wt%-Pt/BZY10 and (**b**) 0.05 wt%-Ru/BZY10.

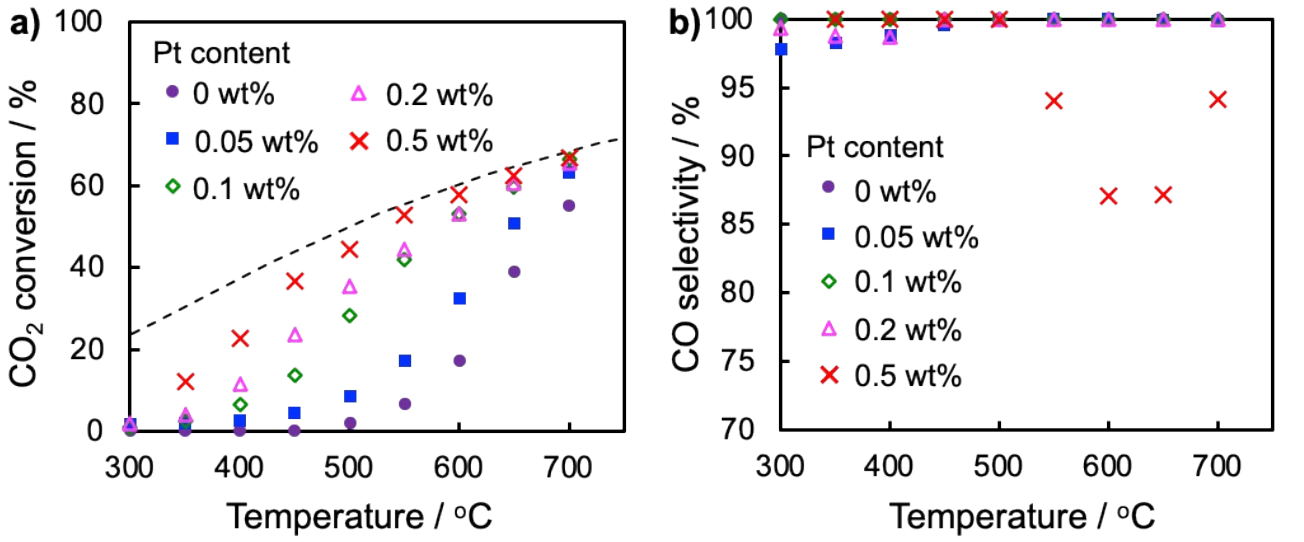

Figure S10. (**a**,**b**) Temperature-dependent (**a**) CO_2 conversion and (**b**) CO selectivity on the CO_2 hydrogenation under the gas stream of H_2/CO_2 = 3 over Pt/BZY10 with different Pt content (0.00, 0.05, 0.10, 0.20, and 0.50 wt%).